Developing Image-based Search Capabilities Within Hospital Databases to Diagnose Rare Brain Tumors

Nazanin Maleki, MD, Research Fellow, Radiology, The Children's Hospital of Philadelphia
Sahil Chadha, MD; Marc von Reppert, MD; Klara Willms, MD; Arman Avesta, MD, PhD; Tal Zeevi, PhD; MingDe Lin, PhD; Karl-Titus Hoffmann, MD; Sanjay Aneja, MD; Mariam Aboian, MD, PhD

Introduction

Current neuroradiology reference materials don't fully capture the wide variety of brain tumor appearances, and text-based image search tools struggle due to inconsistent radiology report formats. previous studies attempting to create image-based search tools for brain tumor MRIs faced practical challenges. Techniques like feature extraction, image fusion, and transfer learning were explored, but these required expert neuroradiologists to manually delineate tumors, making them too complicated for routine clinical use. Additionally, previous algorithms didn't involve clinicians in validating the usefulness of the search results, and they lack accurate matching of specific brain tumor subtypes. There has been a gap in addressing brain tumor subtype classification with greater precision in retrieval.

Hypothesis

An automated image-based search pipeline integrating convolutional neural networks and dimensionality reduction can efficiently retrieve clinically relevant brain tumor cases with high precision, improving diagnostic support and educational resources.

Methods

295 patients (mean age and SD, 51 ± 20 years) with primary brain tumors who underwent surgical and/or radiotherapeutic treatment between 2000 and 2021 were included in this retrospective study. Semi-automated convolutional neural network-based tumor segmentation was performed, and radiomic features were extracted. The dataset was split into reference and query subsets, and four dimensionality reduction techniques including PCA, t-SNE, UMAP, and PHATE were applied to cluster reference cases. Radiomic features extracted from each query case were projected onto the clustered reference cases, and nearest neighbors were retrieved. Retrieval performance was evaluated using mean average precision at k, and the best-performing dimensionality reduction technique was identified. four expert neuroradiologists independently rated visual similarity using a five-point Likert scale.

Results

t-SNE with six components was the highest-performing dimensionality reduction technique, with mean average precision at 5 ranging from 78% to 100% by tumor type. PCA and UMAP achieved comparable results to t-SNE for Glioblastoma,Astrocytoma, and Meningioma, but results differed for Pilocytic Astrocytoma. PCA achieved a maximum mAP@5 of 73% for PA, and UMAP achieved 68%, compared to 78% for t-SNE. Across tumor types, the poorest performance was observed for PHATE. The top five retrieved reference cases showed high visual similarity Likert scores with corresponding query cases (76% 'similar' or 'very similar').

Conclusion

There is a critical need for a method to retrieve historical medical images based on visual similarity to an image query. We introduce an image-based search algorithm that automatically retrieves similar reference cases based on extracted query image features without any text input and this algorithm is the first to separate glioma subtypes.

Figure(s)

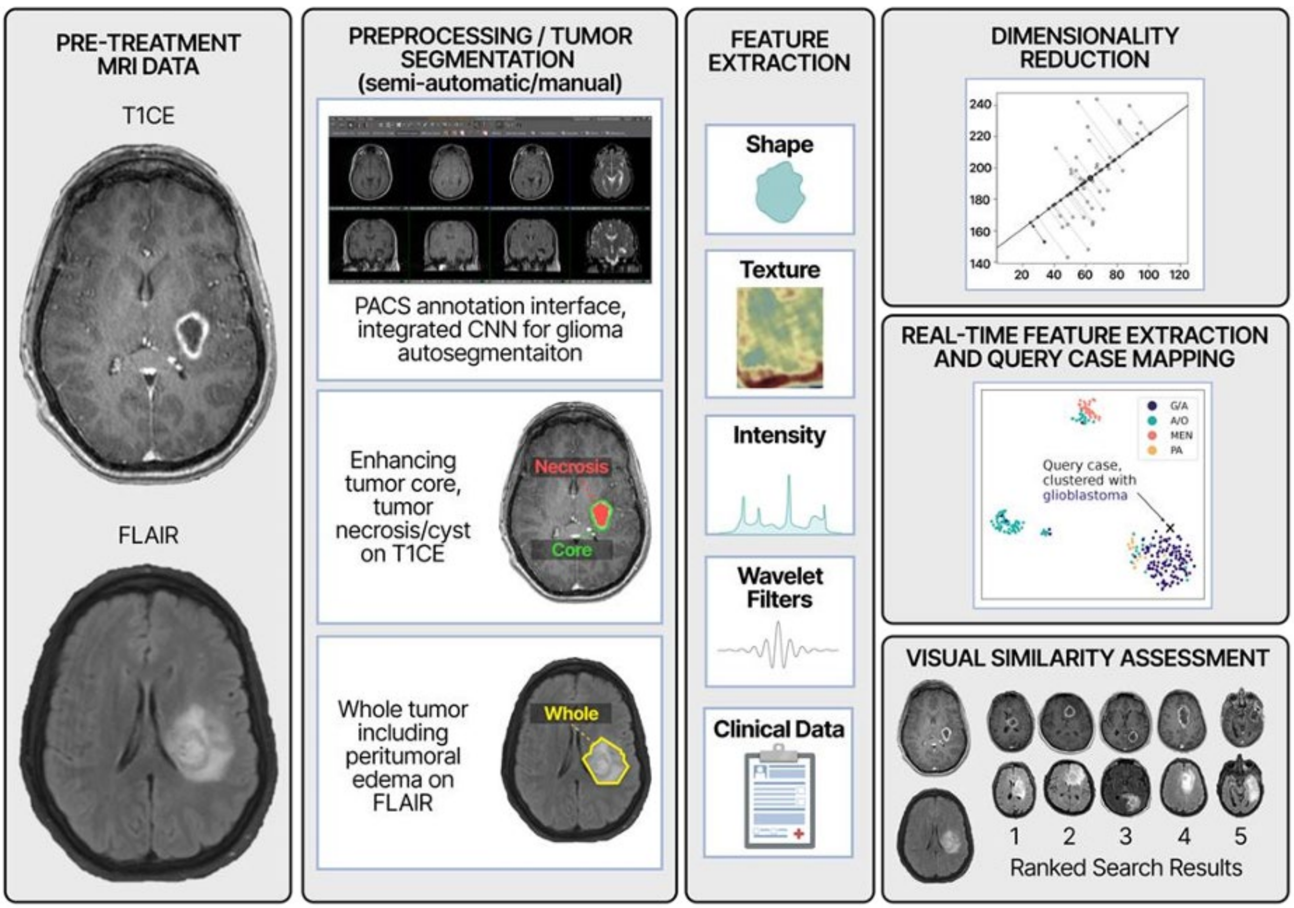

Figure 1. PACS-integrated Workflow for Volume of Interest Segmentation, Feature Extraction, Dimensionality Reduction and Clustering of Query Case. The inputs to our workflow are fluid attenuated inversion recovery (FLAIR) and T1-weighted contrast-enhanced (T1CE) images. Semi-automated segmentation was performed within our PACS to segment the whole, enhancing, and necrotic/cystic components of the tumor. Then, 788 radiomic features were extracted from the segmented tumor components. These extracted radiomic features additionally underwent wavelet transformation and were combined with clinical data, including age and sex. Dimensionality reduction was subsequently performed on these features. Reference cases were then projected into dimensionality-reduced space, clustering similar cases together. Finally, for a query case, the nearest reference cases in the dimensionality-reduced space were identified.

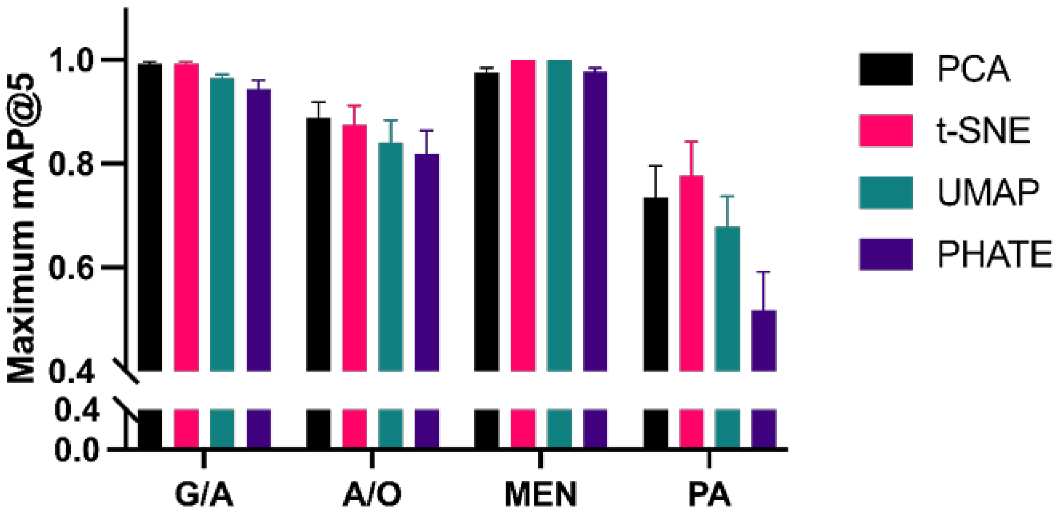

Figure 2. Maximum Mean Average Precision of Top 5 Retrieved Cases by Dimensionality Reduction Technique and Tumor Type. Error bars represent standard errors of the mean. PCA indicates Principal Component Analysis; t-SNE, t-Distributed Stochastic Neighbor Embedding; UMAP, Uniform Manifold Approximation and Projection; PHATE, Potential of Heat-Diffusion for Affinity-Based Trajectory Embedding. G/A indicates glioblastoma and astrocytoma CNS World Health Organization grade 4; A/O, astrocytoma and oligodendroglioma CNS World Health Organization grades 2-3; MEN, meningioma; PA, pilocytic astrocytoma.

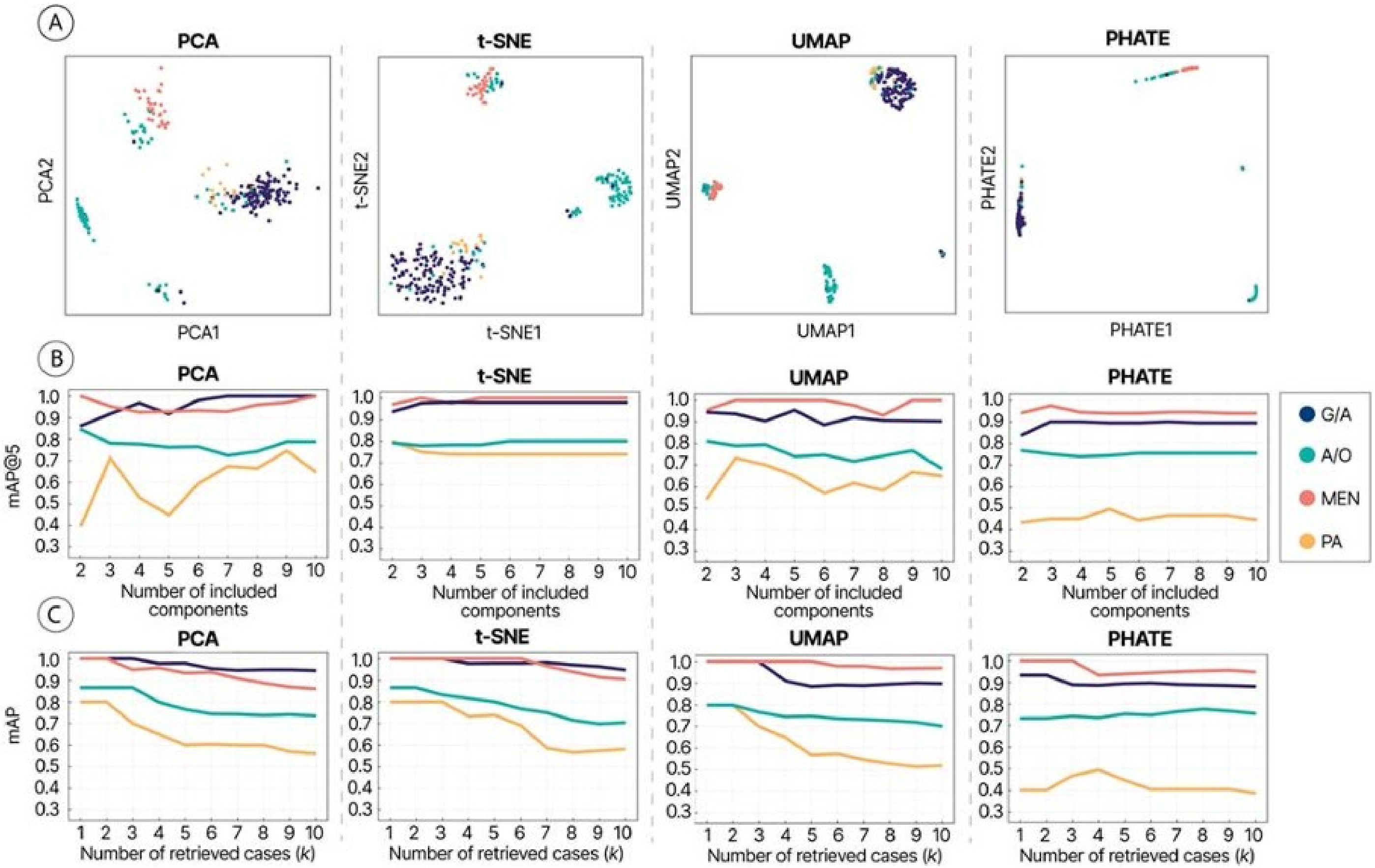

Figure 3. Retrieval Case Clustering and Performance. A, Retrieval case clustering of the first two components. B, mean average precision at 5 by varying number of components. C, mean average precision at k for six included components and varying number of retrieved cases (k). t-SNE indicates t-Distributed Stochastic Neighbor Embedding; PCA, Principal Component Analysis; UMAP, Uniform Manifold Approximation and Projection; PHATE, Potential of Heat-Diffusion for Affinity-Based Trajectory Embedding. G/A indicates glioblastoma and astrocytoma CNS World Health Organization grade 4; A/O, astrocytoma and oligodendroglioma CNS World Health Organization grades 2-3; MEN, meningioma; PA, pilocytic astrocytoma.

Keywords

Artificial Intelligence/Machine Learning; Educational Systems; Imaging Research